Feasibility of large-scale power plants based on thermoelectric effects

2014 New J. Phys. 16 123019

(http://iopscience.iop.org/1367-2630/16/12/123019)

New Journal of Physics
The open access journal at the forefront of physics
Deutsche Physikalische Gesellschaft DPG | IOP Institute of Physics

Feasibility of large-scale power plants based on thermoelectric effects

Liping Liu
Department of Mechanical Aerospace Engineering, Rutgers University, Piscataway, NJ 08854, USA
Department of Mathematics, Rutgers University, Piscataway, NJ 08854, USA
E-mail: liu.liping@rutgers.edu

Received 9 July 2014, revised 29 October 2014
Accepted for publication 31 October 2014
Published 8 December 2014
New Journal of Physics **16** (2014) 123019
doi:10.1088/1367-2630/16/12/123019

Abstract
Heat resources of small temperature difference are easily accessible, free and enormous on the Earth. Thermoelectric effects provide the technology for converting these heat resources directly into electricity. We present designs for electricity generators based on thermoelectric effects that utilize heat resources of small temperature difference, e.g., ocean water at different depths and geothermal resources, and conclude that large-scale power plants based on thermoelectric effects are feasible and economically competitive. The key observation is that the power factor of thermoelectric materials, unlike the figure of merit, can be improved by orders of magnitude upon laminating good conductors and good thermoelectric materials. The predicted large-scale power generators based on thermoelectric effects, if validated, will have the advantages of the scalability, renewability, and free supply of heat resources of small temperature difference on the Earth.

Keywords: thermoelectric, power factor, energy conversion

1. Introduction

By the second law of thermodynamics, heat, as a form of energy, can be converted into usable energy only if there is a temperature difference between two heat reservoirs. The ideal

efficiency of conversion is given by the Carnot efficiency:

$$\eta_{\text{Carnot}} = \frac{T_{\text{h}} - T_{\text{c}}}{T_{\text{h}}}, \tag{1}$$

where T_{h} and T_{c} are the high and low temperature, respectively. From this viewpoint, the largest accessible energy reservoir on Earth is undoubtedly the oceans, stemming from the thermocline in oceans: the surface water temperature within a hundred meters of sea level is around 20 K higher than that below 600 m in tropical regions, since the surface water is heated by, stores and concentrates solar energy. If this energy resource can be converted to electricity at a competitive cost, even at a fraction of the ideal Carnot efficiency, it may provide an important avenue to solving the world's energy problems.

The conventional technology of large-scale power plants using chemical or nuclear fuels has to first convert heat into kinetic energy, which is then used to propel electromagnetic power generators. Because of the small temperature difference in ocean water or geothermal resources, this two-stage conversion technology has to use ammonia, among other things, as a working fluid and generates electricity by means of a low pressure turbine. This concept of 'ocean thermal energy conversion' (OTEC) was envisioned more than 130 years ago by d'Arsonval in the 1880s; experimental OTEC facilities have been built since 1930 [1, 2]. Currently, an OTEC plant is operating in Japan, with several OTEC power plants proposed in the US and China [3].

Thermoelectric (TE) materials, on the other hand, can directly convert heat into electricity no matter how small the temperature difference is [4]. Small-scale TE generators have been commercialized in applications in: microelectronics, for reliable and independent power supply [5, 6]; automobiles, for improving overall fuel efficiency [7]; and producing electricity in remote areas [8]. In conventional designs, the efficiency of conversion is a predominant design criterion for controlling cost, since fuels account for the major cost of power generation [9–14]. The efficiency of a TE generator is dictated by a material property, namely, the dimensionless figure of merit, which, to the best of our knowledge, is hard to improve. The state-of-the-art TE materials have a dimensionless figure of merit of around 2.4 at room temperature [11, 15], corresponding to an efficiency that is about 20% of the ideal Carnot efficiency. In practice, commercial products use TE materials with figure of merit below 1 and hence have an overall device efficiency of around 5% to 10% of the ideal Carnot efficiency. A larger dimensionless figure of merit is necessary for large-scale TE generators to be competitive against conventional conversion methods if fuels are consumed, which has motivated recent renewed interest in thermoelectric materials focusing on improving the conversion efficiency.

Here we present a design for power generators based on thermoelectric effects that use the small temperature difference in ocean water as the 'fuel', and show that they are physically feasible and may be economically competitive. The heat resources are taken as free and unlimited, e.g., ocean water at different depths (figure 1, [16]), geothermal sources (figure 2, [17]), or waste heat from conventional power plants [18]. The main cost of the electricity generation therefore comes from the materials, the processes of fabrication and assembly of the generator, and possibly the energy needed to drive the flows for heat exchange and electricity generation. This cost basis, as will be shown below, is realistic and shifts the importance of the conversion efficiency (figure of merit) to that of the conversion capacity (power factor), and favors simple structures for ease of mass production. Power factors of thermoelectric materials, unlike the figure of merit, can be improved by orders of magnitude through engineering thermoelectric structures, e.g., laminating two or more TE materials. An early account of

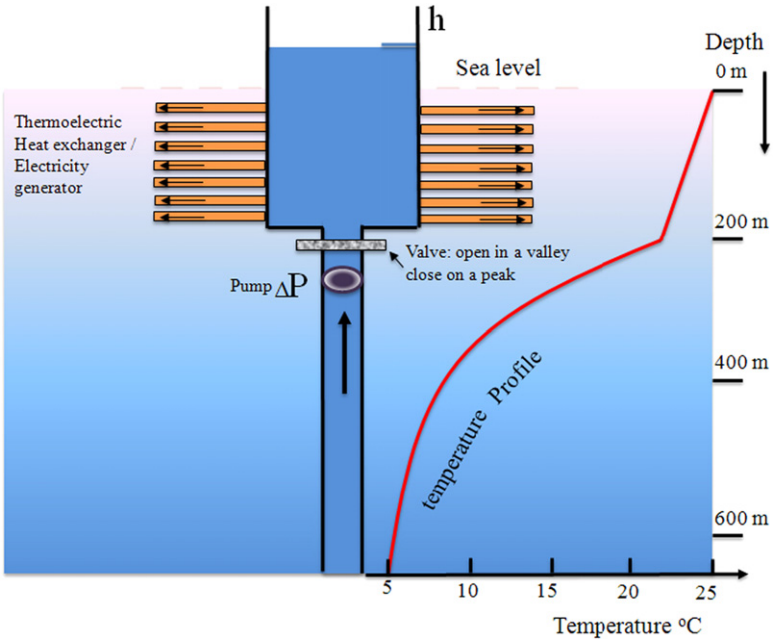

Figure 1. A thermoelectric power plant using the temperature difference of ocean water at different depths: cold water is pumped and passes through the heat exchanger/ generator where it is heated by surface water and generates electricity. The energy of ocean waves can be harvested to drive the flows. Surface water has higher temperature since it absorbs, stores and concentrates sunlight energy. The temperature profile is sketched according to [16], for tropical regions.

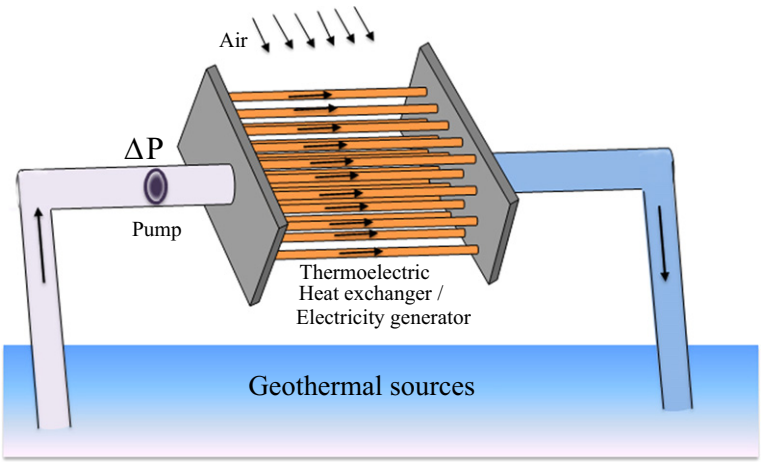

Figure 2. A thermoelectric generator using geothermal resources. Hot water is pumped and passes through the heat exchanger, where it is cooled by air and generates electricity.

thermoelectric composites has been presented in [19, 20], where it has been shown that the power factors of TE composites can be improved via composites. Recently, there have been a number of studies on heterogeneous thermoelectric composites including nonlinear layered TE composites [21, 22], linear particulate TE composites [23], and nonlinear core–shell composites [24]. These studies underscore our claim that the effective power factors of TE composites can indeed be improved significantly via a careful design of composite microstructures.

Below, we focus our analysis on large-scale ocean-based TE power plants using water at different depths as the 'fuel', for renewability and scalability. As illustrated in figure 1, cold water is pumped and driven through tubes in a heat exchanger, where it is heated by surface water. The tubes are made of TE materials, and therefore, as the heat exchanges across the TE tube walls, electricity is generated. In spite of the well-known shortcoming of low conversion efficiency, large-scale ocean-based TE power plants enjoy the following unique and unprecedented advantages:

(i) Heat resources of small temperature difference, i.e., water at deep sea levels (below 600 m), are easily accessible, free and unlimited. The power cost of pumping water and driving the flows can be made free by harvesting energy from ocean waves. A valve can be designed to open in a valley (below sea level) and close on a peak (above sea level) of ocean waves, and subsequently an average water height above sea level in the cold water tank can be maintained without any power cost.

(ii) It costs no land and can be installed in three dimensions, and hence has superior scalability.

(iii) It is green, it is reliable as there are no moving solid parts, and it has low maintenance cost.

(iv) The power output is independent of the hour of the day and season at a tropical site.

In addition we notice that ocean waves and convection naturally mix surface water, and hence no power is needed to drive the flows exterior to the heat exchanger, and that there is no stringent structural requirement on the long underwater pipe if the material density is close to that of water. Structural materials of this kind can be realized from reinforced foam or plastics at a low cost, and these materials also serve as good thermal insulators.

2. Proposed designs for the TE generator

2.1. The flow problem

Below, we show that large-scale ocean-based TE power plants at the megawatt order are feasible and economically competitive even if power is needed to pump water and drive the flows on a waveless day. To this end, we first estimate the amount of energy lost in maintaining continuous flow in a system that includes the underwater pipe and TE tubes, shown in figure 1.

For simplicity, we assume that the flows in the underwater pipe and TE tubes are steady and laminar, with a low Reynolds number ($Re < 2300$). For a circular pipe of length L and radius R and a pressure drop ΔP , the flow problem is referred to as the Hagen–Poiseuille flow in classic fluid dynamics. By the Navier–Stokes equation, the flow velocity $v = v(r)$ will satisfy [25]:

$$\begin{cases} \mu \dfrac{1}{r}\dfrac{\mathrm{d}}{\mathrm{d}r} r \dfrac{\mathrm{d}}{\mathrm{d}r} v(r) - p' = 0 & \text{if } r \in [0, R), \\ v(r) = 0 & \text{if } r = R, \end{cases}$$

where μ is the viscosity of water at 293 K and $p' = -\Delta P/L$ is the pressure gradient. The solution to the above problem is given by

$$v(r) = \frac{\Delta P \left(R^2 - r^2\right)}{4\mu L},$$

and henceforth the volumetric flow rate is given by

$$Q = \int_0^R v(r) 2\pi r \mathrm{d}r = \frac{\pi \Delta P R^4}{8\mu L}. \tag{2}$$

The power dissipated by the viscosity is given by

$$P^d = \int_0^L \int_0^R \mu |\nabla v|^2 2\pi r \mathrm{d}r \mathrm{d}x = \frac{\pi \Delta P^2 R^4}{8\mu L} =: \mu \gamma L Q^2 / A^2, \tag{3}$$

where A is the cross-sectional area and $\gamma = 8\pi$ for a circular pipe.

From (3), we see that the power needed to pump water to a height h and the flow rate through TE tubes driven by a pressure $\rho g h$ are given by

$$\begin{aligned} P_{\text{loss}} &= \mu\, \gamma_{\text{pp}} N_{\text{pp}} L_{\text{pp}} \frac{Q_{\text{pp}}^2}{A_{\text{pp}}^2} + \mu\, \gamma_{\text{tb}} N_{\text{tb}} L_{\text{tb}} \frac{Q_{\text{tb}}^2}{A_{\text{tb}}^2}, \\ Q_{\text{tb}} &= \frac{\rho g h A_{\text{tb}}^2}{\mu \gamma_{\text{tb}} L_{\text{tb}}}, \end{aligned} \tag{4}$$

where $\mu = 1.0 \times 10^{-3}$ Pa s ($\rho = 10^3\,\mathrm{kg\,m^{-3}}$) is the viscosity (density) of water, N_{pp} (N_{tb}) is the number of underwater long pipes (near-surface short TE tubes), L_{pp} and A_{pp} (L_{tb} and A_{tb}) are the length and cross-sectional area of the pipe (TE tube), Q_{pp} (Q_{tb}) is the volumetric rate of flow through the pipe (TE tube), and γ_{pp} (γ_{tb}) is a dimensionless geometric factor depending on the cross-sectional shape of the pipe (TE tube). If both are circular, $\gamma_{\text{pp}} = \gamma_{\text{tb}} = 8\pi$. Further, $N_{\text{pp}} Q_{\text{pp}} = N_{\text{tb}} Q_{\text{tb}} = Q$ is the total volumetric rate of flow through the generator, the second term in P_{loss} can be identified as $\rho g h Q$, and P_{loss} scales as $1/N_{\text{pp}}$ and $1/N_{\text{tb}}$ for fixed Q. The formula (4) underestimates the actual power loss by neglecting turbulence, friction with the pipe/tube walls, etc, but is accurate at the order of magnitude and sufficient for our subsequent analysis.

2.2. The thermoelectric problem

The TE tubes (constituting the generator) are submerged in high temperature surface water. As the cold water flows through the TE tubes, the temperature difference between the interior wall and the exterior wall of the TE tube results in heat transfer across the TE tube walls and direct thermal-to-electric energy conversion. Electrically, the TE tube may be divided into multiple segments to boost the electric potential difference and power output, as illustrated in figure 3(a), (b); the detailed design of the electric connection is beyond the scope of this paper and will not be discussed below.

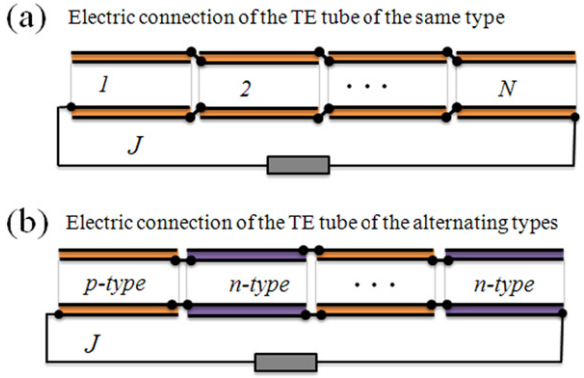

Figure 3. (a) Electric connection of the TE tube in the longitudinal direction if the type of TE material remains the same. (b) Electric connection of the TE tube in the longitudinal direction for alternating kinds of TE materials.

To estimate the electric energy gain from the TE tubes, we now consider the thermoelectric problem as water flows through the TE tube immersed in an ambient medium of 10 K temperature difference. For simplicity, assume that each segment of tube is short enough that the temperature and electric potential on the interior and exterior walls may be regarded as constant on each segment; see figure 3(a), (b). Further, it is desirable that each segment of the TE tube works at the optimal conditions for having maximum power generation per unit volume, i.e., the segment length l_i and the total electric current J will be controlled such that the electric current density across the wall of each segment is given by (cf. section 3.1.1 of Liu (2012))

$$j_{\mathrm{e}}(x) = \frac{s\sigma\left(T_{\mathrm{ex}} - T(x_i)\right)}{2t_{\mathrm{tb}}}, \tag{5}$$

where s is the Seebeck coefficient of the TE materials, T_{ex} is the temperature of the exterior walls of all TE tubes, and x_i is the midpoint of the ith segment. Since the electric current in the closed circuit is constant, the length of each segment l_i will be proportional to $1/(T_{\mathrm{ex}} - T(x_i))$. Under these conditions, the efficiency of the conversion is suboptimal and is given by (T_0 is the average temperature)

$$\eta = \eta_{\mathrm{s}}\eta_{\mathrm{Carnot}}, \qquad \eta_{\mathrm{s}} = \frac{ZT_0}{4 + 2ZT_0}, \tag{6}$$

which is only 0.5% less than the optimal efficiency $\eta_{\mathrm{s}}^{\mathrm{opt}} = (\sqrt{ZT_0 + 1} - 1)/(\sqrt{ZT_0 + 1} + 1)$ for $ZT_0 = 1$, and even smaller for smaller ZT_0. Also, the potential difference between exterior and interior walls at the ith segment is given by

$$\mu_{\mathrm{ex}}(x_i) - \mu_{\mathrm{in}}(x_i) = -\frac{s}{2}\left(T_{\mathrm{ex}} - T(x_i)\right) \quad (i = 1, \ldots, N). \tag{7}$$

The reader is invited to check for the details of above results in Liu (2012 [23]).

Moreover, the heat flux flowing out of the tube across the tube wall is given by

$$q(x) = -\kappa_q \frac{T_{\mathrm{ex}} - T(x)}{t_{\mathrm{tb}}}, \quad \kappa_q = \kappa + T_0\sigma s^2/2, \tag{8}$$

where κ (σ) is the thermal (electric) conductivity of the TE tube wall. For simplicity we assume that the length of the tube is much larger than the cross-sectional diameter of the tube, and hence the temperature may be approximately regarded as uniform on each cross-section of the tube. Neglecting the heat generated by the viscosity, by the energy balance we have

$$\rho C_p Q_{\rm tb} \frac{\rm d}{{\rm d}x} T(x) + l_{\rm tb} q(x) = 0, \tag{9}$$

where $C_p = 4.18 \times 10^3\ {\rm J\,kg^{-1}\ K^{-1}}$ is the specific heat of water and $l_{\rm tb}$ is the length of the interior perimeter of the TE tube. Taking account of the inlet temperature $T(x=0) = T^0$, which may be assumed to be the temperature of the source, by (8) and (9) we have

$$T(x) = T_{\rm ex} + \left(T^0 - T_{\rm ex}\right) \exp\left(-x/L_*\right), \qquad L_* = \frac{\rho C_p Q_{\rm tb} t_{\rm tb}}{\kappa_q l_{\rm tb}}. \tag{10}$$

Therefore, the outlet temperature is given by

$$T\left(L_0\right) = T_{\rm ex} + {\rm e}^{-\lambda/2}\left(T^0 - T_{\rm ex}\right), \qquad \lambda = \frac{2L_{\rm tb}}{L_*} = \frac{2\kappa_q l_{\rm tb} L_{\rm tb}}{\rho C_p Q_{\rm tb} t_{\rm tb}}. \tag{11}$$

The power generated by each tube is the sum of the powers generated by all of the segments and well approximated by (cf section 3.1.1 in Liu (2012))

$$P_{\rm out} = \int_0^{L_{\rm tb}} \frac{P_{\rm f}}{4} \frac{\left(T(x) - T_{\rm ex}\right)^2}{t_{\rm tb}^2} t_{\rm tb} l_{\rm tb} {\rm d}x = \frac{P_{\rm f} \delta T^2 l_{\rm tb} L_{\rm tb}}{4 t_{\rm tb}} \cdot \frac{1 - \exp(-\lambda)}{\lambda},$$

where $P_{\rm f} = \sigma s^2$ is the power factor of the TE material. Therefore, taking account of the power loss $P_{\rm loss}$ (cf (4)), the power gain from each TE tube is given by

$$P_{\rm gain} = P_{\rm out} - \mu\, \gamma_{\rm tot} L_{\rm tb} \frac{Q_{\rm tb}^2}{A_{\rm tb}^2} = \frac{P_{\rm f} \delta T^2 l_{\rm tb} L_{\rm tb}}{4 t_{\rm tb}} f(\lambda, \beta), \tag{12}$$

where

$$\gamma_{\rm tot} = \gamma_{\rm tb} + \frac{\gamma_{\rm pp} L_{\rm pp} A_{\rm tb}^2 N_{\rm tb}}{\gamma_{\rm tb} L_{\rm tb} A_{\rm pp}^2 N_{\rm pp}}, \qquad \beta = \gamma_{\rm tot} \frac{16 \mu \kappa_q^2}{\rho^2 C_p^2 P_{\rm f}\ \delta T^2} \cdot \frac{L_{\rm tb}^2 l_{\rm tb}}{t_{\rm tb} A_{\rm tb}^2}$$

$$\lambda = \gamma_{\rm tb} \frac{2\mu\kappa_q}{C_p \rho^2\ g} \cdot \frac{1}{h} \cdot \frac{l_{\rm tb} L_{\rm tb}^2}{t_{\rm tb} A_{\rm tb}^2} = \frac{1}{h} \cdot \frac{\gamma_{\rm tb}}{\gamma_{\rm tot}} \cdot \frac{C_p P_{\rm f}\ \delta T^2}{8 \kappa_q g} \beta$$

and

$$f(\lambda, \beta) = \frac{1 - \exp(-\lambda)}{\lambda} - \frac{\beta}{\lambda^2}. \tag{13}$$

2.3. Optimal designs

From equation (12), it is clear that a large power factor $P_{\rm f}$ is crucial for improving $P_{\rm gain}$. The power factor can be significantly improved by using composites. To see this, we consider laminates of two materials, as illustrated in figure 4(a). From the definition $P_{\rm f} = \sigma s^2$, we see that the power factor will be improved if the electric conductivity increases while the Seebeck

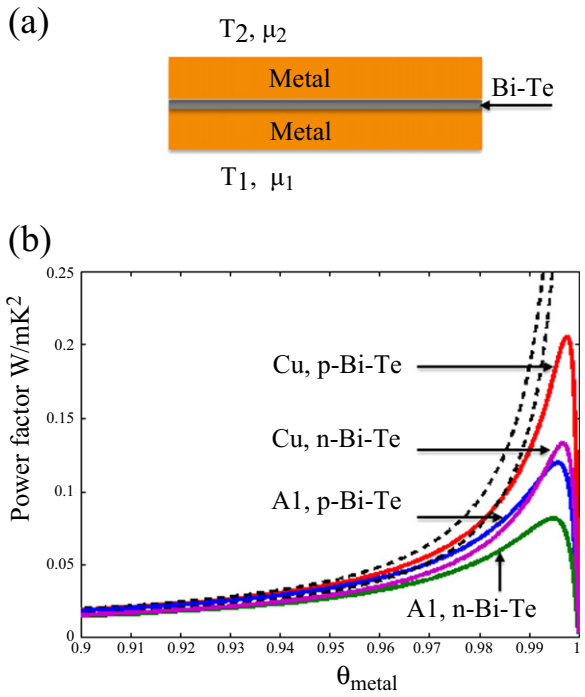

Figure 4. Power factors of simple laminates of two materials: (a) a sketch of the laminate; and (b) the power factor as a function of the volume fraction of the metal. The solid curves are plotted according to the self-consistent continuum theory, i.e., (13); the dashed lines are plotted according to the rough estimate (14). There is no discernible difference between the two predictions for lower volume fraction of the metal.

coefficient s is maintained. We therefore consider laminates of good conductors, e.g., Cu ($\sigma = 5.85 \times 10^7\,\Omega^{-1}\,\mathrm{m}^{-1}$, $\kappa = 401\,\mathrm{W\,m^{-1}\,K^{-1}}$, $s = 1.90\,\mu\mathrm{V\,K^{-1}}$) or Al ($\sigma = 3.66 \times 10^7\,\Omega^{-1}\,\mathrm{m}^{-1}$, $\kappa = 237\,\mathrm{W\,m^{-1}\,K^{-1}}$, $s = -1.66\,\mu\mathrm{V\,K^{-1}}$) [11], with TE materials with large Seebeck coefficients, e.g., Bi–Te semiconductor systems composed of p-type-doped $(Bi_{0.25}Sb_{0.75})_2Te_3$ ($\sigma = 0.33 \times 10^5\,\Omega^{-1}\,\mathrm{m}^{-1}$, $\kappa = 0.559\,\mathrm{W\,m^{-1}\,K^{-1}}$, $s = 245\,\mu\mathrm{V\,K^{-1}}$) or n-type-doped $Bi_2(Te_{0.94}Sb_{0.06})_3$ ($\sigma = 0.36 \times 10^5\,\Omega^{-1}\,\mathrm{m}^{-1}$, $\kappa = 0.788\,\mathrm{W\,m^{-1}\,K^{-1}}$, $s = -209\,\mu\mathrm{V\,K^{-1}}$) [26].

Since the electric conductivity and thermal conductivity differ between the metals and semiconductors by more than two orders of magnitude, for the applied boundary conditions illustrated in figure 4(a) we anticipate the electric potential and temperature drop to occur mainly across the semiconductor layer, and hence the Seebeck coefficient remains roughly that of the semiconductor, i.e., the effective Seebeck coefficient $s^{\mathrm{e}} = s_{\mathrm{sm}}$. For uncoupled electric or thermal conductivity problems, it is classical that the effective conductivities of laminates are given by

$$\sigma^{\mathrm{e}} = \left(\frac{\theta_{\mathrm{mt}}}{\sigma_{\mathrm{mt}}} + \frac{\theta_{\mathrm{sm}}}{\sigma_{\mathrm{sm}}}\right)^{-1}, \qquad \kappa^{\mathrm{e}} = \left(\frac{\theta_{\mathrm{mt}}}{\kappa_{\mathrm{mt}}} + \frac{\theta_{\mathrm{sm}}}{\kappa_{\mathrm{sm}}}\right)^{-1},$$

and hence the effective power factor is given by

$$P_{\mathrm{f}}^{\mathrm{e}} = \sigma^{\mathrm{e}}\left(s^{\mathrm{e}}\right)^2 = \left(\frac{\theta_{\mathrm{mt}}}{\sigma_{\mathrm{mt}}} + \frac{\theta_{\mathrm{sm}}}{\sigma_{\mathrm{sm}}}\right)^{-1} (s_{\mathrm{sm}})^2, \tag{14}$$

where θ_{mt} and θ_{sm} are the volume fractions of the metal and semiconductor in the laminate, respectively. The above formula predicts that the power factor would increase significantly if θ_{mt} increased, since σ^{e} increases monotonically from that of the semiconductor to that of the metal as θ_{mt} increases from 0 to 1.

Equation (14) is accurate when θ_{mt} is not close to 1. On the other hand, it is desirable to have θ_{mt} close to 1 to improve the power factor as much as possible. Taking account of the electric and thermal couplings, a continuum theory for TE materials has been systematically developed in Liu (2012), where the effective TE properties of the laminate are predicted as

$$\begin{bmatrix} T_0\sigma^{\mathrm{e}} & T_0^2\sigma^{\mathrm{e}}s^{\mathrm{e}} \\ T_0^2\sigma^{\mathrm{e}}s^{\mathrm{e}} & T_0^2\left[\kappa^{\mathrm{e}} + T_0\sigma^{\mathrm{e}}\left(s^{\mathrm{e}}\right)^2\right] \end{bmatrix} = \left\{ \theta_{\mathrm{mt}} \begin{bmatrix} T_0\sigma_{\mathrm{mt}} & T_0^2\sigma_{\mathrm{mt}}s_{\mathrm{mt}} \\ T_0^2\sigma_{\mathrm{mt}}s_{\mathrm{mt}} & T_0^2\left[\kappa_{\mathrm{mt}} + T_0\sigma_{\mathrm{mt}}(s_{\mathrm{mt}})^2\right] \end{bmatrix}^{-1} \right.$$
$$\left. + \theta_{\mathrm{sm}} \begin{bmatrix} T_0\sigma_{\mathrm{sm}} & T_0^2\sigma_{\mathrm{sm}}s_{\mathrm{sm}} \\ T_0^2\sigma_{\mathrm{sm}}s_{\mathrm{sm}} & T_0^2\left[\kappa_{\mathrm{sm}} + T_0\sigma_{\mathrm{sm}}(s_{\mathrm{sm}})^2\right] \end{bmatrix}^{-1} \right\}^{-1}.$$

Figure 4(b) shows the power factors of Cu and p-type-doped $(Bi_{0.25}Sb_{0.75})_2Te_3$, Cu and n-type-doped $Bi_2(Te_{0.94}Sb_{0.06})_3$, Al and p-type-doped $(Bi_{0.25}Sb_{0.75})_2Te_3$, and Al and n-type-doped $Bi_2(Te_{0.94}Sb_{0.06})_3$, each as a function of the volume fraction θ_{mt}. We observe that there is an optimal volume fraction, typically very close to 1, such that the power factor is maximized with the maximum power factor about 100 times that of the constituent semiconductor. In particular, for Cu and p-type-doped $(Bi_{0.25}Sb_{0.75})_2Te_3$, the sandwich laminate has maximum power factor $P_{\mathrm{f}}^{\mathrm{e}} = 0.206$ W m^{-1} K^{-2} ($\sigma^{\mathrm{e}} = 8.30 \times 10^6 \Omega^{-1}\mathrm{m}^{-1}$, $\kappa^{\mathrm{e}} = 158$ W m^{-1} K^{-1}, $s^{\mathrm{e}} = 145$ μV K^{-1}) when $\theta_{\mathrm{Cu}} = 0.9975$. We also remark that the sandwich structure illustrated in figure 4(a) is convenient for mass production and for electric connections, since the metal can serve as electrodes as well.

Moreover, from (12) it is desirable to have a larger factor $f(\lambda, \beta)$. From (13) it is clear that small β is more favorable. We shall assume that $\beta \leqslant 1$, by tuning the geometric factors L_{tb}, l_{tb}, A_{tb}. Upon maximizing $f(\lambda, \beta)$ over $\lambda > 0$ for given β, we obtain the maximum $f_{\max}(\beta)$ and the maximizer $\lambda_{\max}(\beta)$, which are shown in figure 5. From figure 5 we observe that $f_{\max}$ depends on β weakly, varying from 1 to 0.1 when β varies from 10^{-5} to 1. Moreover, by (12) the power gain from each TE tube P_{gain} scales as $1/t_{\mathrm{tb}}$. Therefore, a thin tube wall is preferred and the smallest t_{tb} is limited by the manufacture and structure requirement, which may be reasonably chosen as $t_{\mathrm{tb}} = 0.1$–1 mm.

To fix the design parameters, we select as the TE tube wall material the sandwich laminate of Cu and p-type-doped $(Bi_{0.25}Sb_{0.75})_2Te_3$ with the maximum power factor $P_{\mathrm{f}}^{\mathrm{e}}$. For the maximum power factor, the thickness of the semiconductor layer between metals will be chosen as $t_{\mathrm{sm}} = t_{\mathrm{tb}} \times 0.25\% = 0.25$–$2.5$ μm, which does not appear to be a challenge for the modern technology of nanofabrication. Assume that $\delta T = 10$ K, which suffices to account for the heating up of cold water when it is pumped up from deep sea. Then the dimensionless

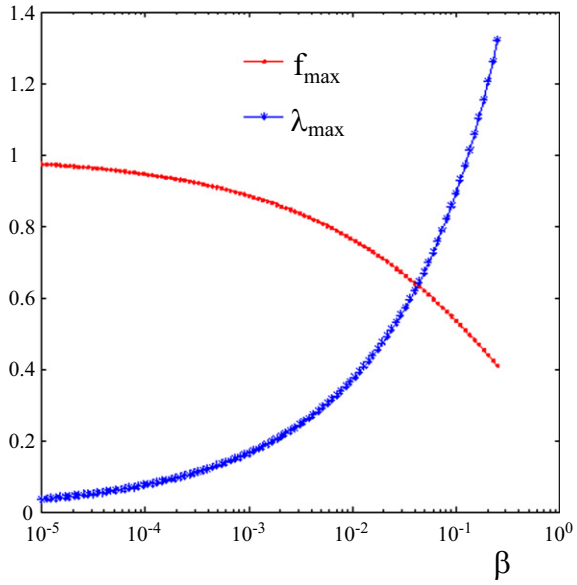

Figure 5. The maximum dimensionless factor $f_{\max}(\beta)$ and the corresponding maximizer $\lambda_{\max}(\beta)$.

Table 1. Proposed designs for a megawatt TE generator ($\delta T = 10$ K).

t_{tb}	R_{tb}	L_{tb}	f_{max}	h	P_{gain}	N_{tb}
0.1	1	1	0.43	1.11	1.39	719
0.2	1	1	0.52	0.75	0.841	1189
0.5	1	1	0.63	0.43	0.408	2453
1	1	1	0.70	0.28	0.227	4415

Physical meanings and dimensions of the symbols: t_{tb}, R_{tb}, L_{tb}: thickness, inner radius and length of the TE tube in mm, cm and m, respectively; f_{max}: maximum dimensionless factor in (12); h in m: the pressure needed to drive the flow in $\rho g h$ (cf figure 1); P_{gain}: the power gain from a tube in kW; N_{tb}: the number of tubes needed for a power gain of one megawatt.

parameters β, λ are given by (SI units)

$$\beta = 1.38 \times 10^{-12} \times \gamma_{tot} \frac{l_{tb} L_{tb}^2}{t_{tb} A_{tb}^2}, \qquad \lambda = \frac{6.28 \gamma_{tb}}{\gamma_{tot}} \times \frac{\beta}{h}.$$

Assume that both the long underwater pipe and the short TE tubes are circular, and select $R_{pp} = 1$ m, $L_{pp} = 10^3$ m, $N_{pp} = 1$, $R_{tb} = 10^{-2}$ m, $L_{tb} = 1$ m, $N_{tb} \leqslant 10^5$, and hence $\gamma_{tot} \approx \gamma_{tb} = 8\pi$, $\beta = 2.21 \times 10^{-5}/t_{tb}$. Upon choosing h such that $\lambda = \lambda_{\max}(\beta)$, we find the power gain $P_{gain} = 0.324 \cdot f_{\max}/t_{tb}$ W from each TE tube, and the number of TE tubes needed for a megawatt power gain listed in table 1. We remark that a rectangular fin-like TE tube may be more favorable in practice for ease of fabrication and mass production; this, however, has little effect on our prediction of the power gain from each TE tube.

3. Conclusion

The estimated cost per year of one megawatt of electricity in 2016 is about 0.83 million USD from conventional coal plants to 1.84 million USD from photovoltaic power plants [27]. Also, the investment in the world's largest photovoltaic farm (Sarnia PV power plant in Canada [28]) is 300 million USD for an annual capacity of 1.2×10^5 MW h, or equivalently, an effective power of 14 megawatts (designed peak power 60 megawatts). Even if table 1 underestimates the number N_{pp} of TE tubes tenfold, it still appears feasible to manufacture a megawatt TE generator using water of 10 K temperature difference as 'fuel', which lasts for 20 years and costs less than 20×1.84 million USD, and is hence economically competitive compared with photovoltaic farms. For geothermal sources, we anticipate the temperature δT to be of the order of 50 K or higher, implying a 25-fold increase of the power gain since P_{gain} scales as δT^2.

In summary, we have presented a simple design for a heat exchanger or electricity generator which uses heat resources of small temperature differences. The theoretical analysis shows that it is feasible and economically competitive to build large-scale ocean-based or geothermal power plants based on thermoelectric effects. A for-the-moment science-fiction vision is that power plant units like barges are manufactured on shore and towed to a selected tropical ocean site where electricity is generated and transmitted to shore. Whenever more power is needed, new units can be manufactured, towed and assembled to the site. The renewability and scalability of the TE power plants may yield a way to resolve the energy crisis facing human societies.

References

[1] Chiles J 2009 The other renewable energy *Invent. Technol.* **23** 24–35

[2] Center C R R 2012 *Ocean Thermal Energy Conversion: Information Needs Assessment* (Durham, NH: University of New Hampshire)

[3] Wikipedia Ocean thermal energy conversion http://en.wikipedia.org/wiki/Ocean-thermal-energy-conversion

[4] DiSalvo F J 1999 Thermoelectric cooling and power generation *Science* **285** 703–6

[5] Leonov V, Torfs T, Fiorini P and Hoof C V 2007 Thermoelectric converters of human warmth for self-powered wireless sensor nodes *IEEE Sens. J.* **7** 650–7

[6] Leonov V and Vullers R J M 2009 Wearable thermoelectric generators for body-powered devices *J. Electron. Mater.* **38** 1491–8

[7] Saqr K M, Mansour M K and Musa M N 2008 Thermal design of automobile exhaust based thermoelectric generators: objectives and challenges *Int. J. Automot. Technol.* **9** 155–60

[8] Nuwayhid R Y, Rowe D M and Min G 2003 Low cost stove-top thermoelectric generator for regions with unreliable electricity supply *Renewable Energy* **28** 205–22

[9] Mahan G D 1998 Good thermoelectrics *Solid State Phys.* **51** 81–157

[10] Yang J, Aizawa T, Yamamoto A and Ohta T 2000 Thermoelectric properties of p-type $(Bi_2Te_3)_x(Sb_2Te_3)_{1-x}$ prepared via bulk mechanical alloying and hot pressing *J. Alloys Compd.* **309** 225–8

[11] Rowe D M (ed) 2006 *Thermoelectrics Handbook: Macro to Nano* (Boca Raton, FL: CRC Press)

[12] Nolas G S, Poon J and Kanatzidis M 2006 Recent Developments in bulk thermoelectric materials *MRS Bull.* **31** 199–205

[13] Snyder G J and Toberer E S 2008 Complex thermoelectric materials *Nat. Mater.* **7** 105–14

[14] Lan Y, Minnich A J, Chen G and Ren Z 2010 Enhancement of thermoelectric figure-of-merit by a bulk nanostructuring approach *Adv. Funct. Mater.* **20** 357–76

[15] Venkatasubramanian R, Siivola E, Colpitts T and O'Quinn B 2001 Thin-film thermoelectric devices with high room-temperature figures of merit *Nature* **413** 597–602
[16] National Oceanic and Atmospheric Administration http://oceanservice.noaa.gov/education/yos/resource/JetStream/ocean/98-sstloop.htm
[17] Department of Energy http://www1.eere.energy.gov/geothermal/maps.html
[18] Hsu C-T, Huang G-Y, Chu H-S, Yu B and Yao D-J 2011 Experiments and simulations on low-temperature waste heat harvesting system by thermoelectric power generators *Appl. Energy* **88** 1291–7
[19] Bergman D J and Levy O 1991 Thermoelectric properties of a composite medium *J. Appl. Phys.* **70** 6821–33
[20] Bergman D J and Fel L G 1999 Enhancement of thermoelectric power factor in composite thermoelectrics *J. Appl. Phys.* **85** 8205–16
[21] Yang Y, Xie S H, Ma F Y and Li J Y 2012 On the effective thermoelectric properties of layered heterogeneous medium *J. Appl. Phys.* **111**
[22] Yang Y, Ma F, Lei C, Liu Y and Li J 2013 Nonlinear asymptotic homogenization and the effective behavior of layered thermoelectric composites *J. Mech. Phys. Solids* **61** 1768–83
[23] Liu L P 2012 A continuum theory of thermoelectric bodies and effective properties of thermoelectric composites *Int. J. Engr. Sci.* **55** 35–53
[24] Yang Y, Gao C and Li J 2014 The effective thermoelectric properties of core-shell composites *Acta Mech.* **225** 1211–22
[25] Fox R W, Pritchard P J and McDonald A T 2008 *Introduction to Fluid Mechanics* (New York: Wiley) ch 8
[26] Yamashita O and Odahara H 2007 Effect of the thickness of Bi-Te compound and Cu electrode on the resultant Seebeck coefficient in touching Cu/Bi-Te/Cu composites *J. Mater. Sci.* **42** 5057–67
[27] Department of Energy, Annual Energy Outlook 2011, December 2010, DOE/EIA-0383, 2010
[28] First Solar 2011 http://www.pv-tech.org/